



HAL
open science

What is the heliopause? Importance of magnetic reconnection and measurement requirements

Benoit Lavraud, M. Opher, K. Dialynas, D L Turner, S. Eriksson, E. Provornikova, M Z Kornbleuth, P. Mostafavi, A. Fedorov, J D Richardson, et al.

► To cite this version:

Benoit Lavraud, M. Opher, K. Dialynas, D L Turner, S. Eriksson, et al.. What is the heliopause? Importance of magnetic reconnection and measurement requirements. *Frontiers in Astronomy and Space Sciences*, 2023, 10, pp.1060618. 10.3389/fspas.2023.1060618 . hal-04274010

HAL Id: hal-04274010

<https://hal.science/hal-04274010>

Submitted on 7 Nov 2023

HAL is a multi-disciplinary open access archive for the deposit and dissemination of scientific research documents, whether they are published or not. The documents may come from teaching and research institutions in France or abroad, or from public or private research centers.

L'archive ouverte pluridisciplinaire **HAL**, est destinée au dépôt et à la diffusion de documents scientifiques de niveau recherche, publiés ou non, émanant des établissements d'enseignement et de recherche français ou étrangers, des laboratoires publics ou privés.

What is the Heliopause? Importance of Magnetic Reconnection and Measurement Requirements

1 **B. Lavraud¹, M. Opher², K. Dialynas³, D. L. Turner⁴, S. Eriksson⁵, E. Provornikova⁴, M. Z.**
2 **Kornbleuth², P. Mostafavi⁴, A. Fedorov⁶, J. D. Richardson⁷, S. A. Fuselier⁸, J. Drake⁹, M.**
3 **Swisdak¹⁰, M. Eubanks⁷, T. Y. Chen¹¹, H. Kucharek¹², P. Kollmann⁴, M. Blanc⁶, N. André⁶, V.**
4 **Génot⁶, R. F. Wimmer-Schweingruber¹³, S. Barabash¹⁴, P. Brandt⁴, and R. McNutt⁴**

5 ¹Laboratoire d'astrophysique de Bordeaux, Univ. Bordeaux, CNRS, Pessac, France

6 ²Department of Astronomy, Boston University, Boston, MA, USA

7 ³Office of Space Research and Technology, Academy of Athens, Athens, Greece

8 ⁴Applied Physics Laboratory, The Johns Hopkins University, Laurel, MD, USA

9 ⁵Laboratory for Atmospheric and Space Physics, Boulder, CO, USA

10 ⁶Institut de Recherche en Astrophysique et Planétologie, Université de Toulouse, CNRS, CNES,
11 Toulouse, France

12 ⁷Massachusetts Institute of Technology, Boston, MA, USA

13 ⁸Southwest Research Institute, San Antonio, TX, USA

14 ⁹Department of Physics, the Institute for Physical Science and Technology and the Joint Space
15 Science Institute, University of Maryland, College Park, MD, USA

16 ¹⁰IREAP, University of Maryland, College Park, MD, USA

17 ¹¹Columbia University, New York, NY, USA

18 ¹²Space Science Center, University of New Hampshire, Durham, NH, USA

19 ¹³Institut fuer Experimentelle und Angewandte Physik, University of Kiel, Kiel, Germany

20 ¹⁴Swedish Institute of Space Physics, Kiruna, Sweden

21 *** Correspondence:**

22 Benoit Lavraud

23 benoit.lavraud@u-bordeaux.fr

24 **Keywords: Heliosphere, Heliopause, Solar wind, Heliosheath, Interstellar medium, Magnetic**
25 **Reconnection, Instrumentation**

26

27

28 **Abstract**

29 We highlight the importance of magnetic reconnection at the heliopause, both as one of the key
 30 processes driving the interaction between solar and interstellar media, but also as an element of the
 31 definition of the heliopause itself. We highlight the main observations that have fed the current
 32 debates on the definition, location and shape of the heliopause. We explain that discriminating
 33 between the current interpretations of plasma and magnetic field structures near the heliopause
 34 necessitates appropriate measurements which are lacking on Voyager 1 and Voyager 2, and describe
 35 some of the ensuing requirements for thermal plasma measurements on a future Interstellar Probe.
 36 The content of this article is also accessible from the Bulletin of the American Astronomical Society
 37 in the framework of the Decadal Survey for Solar and Space Physics 2024-2033 (Lavraud et al.,
 38 2022).

39 **1 Introduction**

40 Launched in 1977, the Voyager 1 and 2 spacecraft, after touring several solar system planets, crossed
 41 the termination shock in 2004 and 2007, respectively, at distances of ~ 94 (Decker et al., 2005; Stone
 42 et al., 2005) and ~ 84 AU (Decker et al., 2008; Stone et al., 2008). Past the termination shock they
 43 observed a previously unexplored reservoir of energetic ions and electrons, the inner heliosheath. A
 44 key population there are pick-up ions (PUIs, produced when neutral particles are ionized by either
 45 solar radiation, charge exchange with solar wind protons or electron impact ionization; e.g., Holzer,
 46 1972; Gloeckler et al., 1994; Zirnstein et al. (2022)). They make up a major part of the plasma
 47 pressure in the heliosheath (Richardson et al., 2008; Zank, 2015; Dialynas et al., 2020; 2022). As
 48 distance increases, a fall-off in outward radial flow should be observed in the heliosheath, consistent
 49 with approaching an interface – the heliopause – where pressure balance should occur between
 50 plasmas and magnetic field of solar and interstellar origins.

51 The crossings of the heliopause into the Very Local Interstellar Medium (VLISM) by Voyager 1 and
 52 2 were then reported to have occurred in 2012 (Webber and MacDonald, 2013; Krimigis et al., 2013;
 53 Stone et al., 2013; Burlaga et al., 2013; Gurnett et al., 2013) and 2018 (Burlaga et al., 2019; Gurnett
 54 and Kurth, 2019; Krimigis et al., 2019; Richardson et al., 2019; Stone et al., 2019) at ~ 122 AU and
 55 ~ 119 AU, respectively. Until then, models often overestimated the distance of the heliopause, placing
 56 it further (up to 30 AU or more) than the actual crossings (Kornbleuth et al., 2021; Kleimann et al.,
 57 2022). Observations showed similar heliopause distances at Voyager 1 and 2 while the termination
 58 shock locations were different by 10 AU. This suggested that the termination shock location is more
 59 variable, likely due to a higher susceptibility to solar variability (e.g., Izmodenov et al., 2009;
 60 Krimigis et al., 2019).

61 Soon after the reported Voyager 1 heliopause crossing, a debate arose as to whether that boundary
 62 was indeed the heliopause (Fisk and Gloeckler, 2014; 2016; 2022; Gloeckler and Fisk, 2015). The
 63 identification of the observed boundary as the heliopause was primarily based on an apparent
 64 depletion in solar type plasma, a depletion in Anomalous Cosmic Rays (ACR) thought to originate at
 65 the termination shock or inner heliosheath (Jokipii and Giacalone 1998; Schwadron and McComas
 66 2006; Strauss et al. 2010), and an abrupt increase in plasma density and Galactic Cosmic Rays (GCR)
 67 of interstellar origin. A large increase in magnetic field strength was also observed, as well as an
 68 unexpected absence of magnetic shear across the heliopause (Burlaga et al., 2013; 2019). Flow
 69 properties also do not fit expectations in the heliosheath, as well as at and beyond the heliopause
 70 (Decker et al., 2012; McComas and Schwadron, 2014; Richardson et al., 2021; 2022; Dialynas et al.,
 71 2021; Fuselier et al., 2021; Cummings et al., 2021).

72 These confounding observations show that the physics governing the location, shape and very nature
73 of the heliopause remains mostly unknown. This largely stems from the lack of appropriate data at
74 both Voyager 1 and 2 for fully characterizing low energy plasma and PUIs, which directly hinders a
75 proper definition of the heliopause. In section 2 we thus first discuss the definition of the heliopause,
76 and then highlight key science questions on the role of magnetic reconnection at the heliopause and
77 the need for low energy plasma measurements in its vicinity and beyond. Phenomena other than
78 magnetic reconnection are of importance at the heliopause, but are not addressed here. Like at other
79 planetary magnetospheres and astrospheres, the Kelvin-Helmholtz, interchange and Rayleigh-Taylor
80 instabilities (Ruderman and Fahr 1993; Florinski et al., 2005; Krimigis et al., 2013; Borovikov and
81 Pogorelov, 2014; Strumik et al., 2014; Zank, 2015; Florinski, 2015; Korolkov et al. 2020, Opher et
82 al., 2021; Dialynas et al., 2021), for instance, have been shown to play important roles at outer
83 heliospheric boundaries, but vast amount of works in many domains over the last decades have
84 shown that magnetic reconnection is ubiquitous in the universe and central to the properties and
85 dynamics of numerous astrophysical objects.

86 **2 Open Science Questions**

87 **2.1 What is the Heliopause?**

88 Taking well-known boundaries at Earth as examples, by construction the plasmopause and
89 magnetopause are well defined. The plasmopause (e.g., Pierrard et al., 2021) is defined as the
90 boundary where a strong gradient in plasma density occurs in the inner magnetosphere such that there
91 are almost no more low energy particles outside of this boundary. It is thus identified based on
92 density measurements. The Earth's magnetopause (e.g., Kivelson and Russell, 1995), by contrast, is
93 defined as a magnetic boundary and thus typically identified using magnetic field data. It is the
94 current sheet that separates regions where either the solar or the terrestrial magnetic field dominates.
95 Importantly, it must be noted that for the magnetopause, because of the occurrence of magnetic
96 reconnection, there are vast amounts of solar plasma penetrating through the boundary and
97 populating large regions of the Earth's magnetosphere at all times (boundary layers, cusp, plasma
98 mantle, etc.). Although there are regions on its inside with plasma from the external medium, the
99 magnetopause is not defined based on which particle populations are observed, but is defined as the
100 outermost current sheet where the magnetic field rotates to become solar-dominated.

101 The term "Heliopause", by contrast, leaves some ambiguity on its definition. It refers to the outer
102 boundary of the heliosphere but does not say if identification should be based on thermal plasma,
103 energetic particles or field observations, and on what signature thereof. Voyager 1 and 2 have clearly
104 entered a region that has much higher plasma density (Gurnett et al, 2013, Gurnett and Kurth 2019),
105 contains significant amounts of interstellar plasma populations (e.g., GCR; Webber and MacDonald,
106 2013), where at least some particle populations of heliospheric origin (e.g., ACR; Webber and
107 MacDonald, 2013) seem to have disappeared and where plasma flows have changed significantly
108 (Richardson et al., 2019, 2021; 2022; Dialynas et al., 2021; Giacalone et al., 2022). The vast majority
109 of the community holds these facts as overwhelming evidence that Voyager 1 and 2 have exited into
110 the VLISM.

111 However, in addition to locations closer than initially predicted by models, the purported heliopause
112 crossings at Voyager 1 and 2 show increases in magnetic field strength higher than expected (but cf.
113 Fuselier and Cairns, 2013; Cairns and Fuselier, 2017), as well as magnetic shears across the
114 heliopause that are much lower than remote observations and models would predict at both spacecraft
115 (Burlaga et al., 2013; 2019). Also, the magnetic field past the heliopause was found to be very stable

116 with unexpectedly high magnetic field and solar-like orientation (Burlaga and Ness 2016), and this
117 remains true to the current day for both Voyager 1 and 2 for many AUs beyond the heliopause. The
118 chances for both spacecraft to have crossed the heliopause, if defined based on magnetic field
119 measurements alone, at locations where the magnetic shear is so low appears extremely unlikely. In
120 addition, recent analyses suggest there exists a radial plasma flow at the heliopause at both Voyager 1
121 and 2, outward from the inner heliosheath out into the VLISM. Such observations are at odds with
122 theoretical expectations for the outer heliosphere and heliopause (Dialynas et al., 2021; Fuselier et
123 al., 2021; Cummings et al., 2021; Richardson et al., 2022), although they are proposed to be
124 consistent with the model of Fisk and Gloeckler (2022), as discussed below. Note, however, that
125 there are instrumental uncertainties with the particle measurements near the heliopause at Voyager 2
126 (Richardson et al., 2021).

127 There is currently no consensus on the interpretation of these magnetic field and flow observations. It
128 points to the lack of appropriate low energy plasma measurements on Voyager 1 and 2, which are
129 critical to determine bulk plasma properties in the few eV to few tens-of-keV range (thermal particles
130 in solar wind, heliosheath, and VLISM, as well as PUIs). We argue in this WP that magnetic
131 reconnection plays a pivotal role in solar-interstellar interaction and in structuring the neighborhood
132 of the heliopause, whatever its definition.

133 **2.2 Where is reconnection occurring on the heliopause, and what are the impacts on large-** 134 **scale topology?**

135 Many recent works have studied the occurrence and impact of magnetic reconnection at the
136 heliopause (e.g., Swisdak et al., 2010; 2013; Fisk and Gloeckler, 2014; 2022; Strumik et al., 2014;
137 Opher et al., 2017; Fuselier and Cairns, 2017; Fuselier et al., 2020; Turner et al., 2022). A prime
138 characteristic of magnetic reconnection is that despite being triggered at small scales (electron and
139 ion scales), it affects the system on a global scale (MHD and much beyond, e.g., the dynamics of
140 whole magnetospheres, solar corona, etc.). In particular, magnetic reconnection allows plasma to
141 protrude across discontinuities that otherwise would be impermeable. A second fundamental impact
142 of magnetic reconnection is that it affects the system's magnetic topology at very large scales (e.g.,
143 Hesse and Cassak, 2020).

144 This latter fact is illustrated in Figure 1a for the Earth's magnetosphere. The context displayed is that
145 of an interplanetary magnetic field (IMF) that has an orientation similar (nearly parallel) to that at the
146 nose of the Earth's magnetosphere. In such a case, the magnetic shear across the magnetopause is
147 low. Magnetic reconnection does not occur near the nose (as it does for southward IMF), but instead
148 occurs at high latitudes above both polar cusps (as marked with blue arrows) and may lead the same
149 IMF field line to reconnect twice with the Earth's magnetic field (green field line labelled (3)).
150 Although reconnection occurs over extended X-lines (out of the plane of the figure), the reconnection
151 region is very small in comparison to the large-scale topological changes that affect the whole
152 dayside magnetopause surface (here the magnetopause is defined as the current sheet separating the
153 solar and Earth's magnetic fields, just inside of field line (3)). This large-scale change in topology
154 leads to significant changes in the plasma properties in the dayside regions. Particles flow across the
155 open magnetopause and form various types of boundary layers on both sides of the current sheet
156 (inside and outside), with signatures of the penetration, disappearance and mixing of populations of
157 various types and energies as a function of time, location, species, etc. These effects are very well
158 documented at Earth (e.g., Gosling et al., 1990).

159 The outer heliospheric system is obviously different, but similarities also exist. This is illustrated in
160 Figure 1b that displays the complex, wound structure of the magnetic field in the outer heliosphere
161 (adapted from Opher et al., 2017). Although Voyager 1 and 2 observations show that the magnetic
162 shear across the heliopause is lower than expected, the magnetic field orientation in the VLISM is
163 expected to have a dominant orientation mostly parallel to that in the inner heliosheath at the nose.
164 For that reason, recent modeling found that reconnection is not expected to occur along the nose
165 (e.g., Swisdak et al., 2010, Fuselier and Cairns, 2017). It is instead expected on the flanks of the
166 heliopause, as marked with blue arrows in Figure 1b. As shown by Opher et al. (2017), in such a
167 configuration the same wound (Parker spiral) heliospheric field line may reconnect twice with the
168 VLISM at widely separated locations (blue reconnection regions marked with arrows). Because it
169 allows the same field lines to reconnect twice, this process bears an interesting resemblance with the
170 Earth's magnetosphere under northward IMF, as depicted in Figure 1a. As explained next, such
171 topologies would mean that there exists complex, intricate signatures in particle and field
172 measurements in the vicinity of the heliopause (cf. Fuselier and Cairns (2017) for instance).

173 Figure 1a illustrates the complex signatures expected in suprathermal electron flow (i.e., pitch angle)
174 anisotropies at Earth. Toward the top of Figure 1a, next to field lines numbered (1 - black), (2 - blue)
175 and (3 - green) the small blue and red vectors highlight pristine (i.e., rather cold) and heated,
176 respectively, suprathermal electron flows. Heated electrons are the signature of the spacecraft being
177 located on a reconnected field line, and the direction of the suprathermal electron flow signals the
178 direction of the reconnection region. The small red arrows pointing northward next to field lines (2)
179 and (3) at the top of Figure 1a signal the fact that reconnection has occurred southward along those
180 field lines. However, the reconnection region may very well be at a very distant location (given the
181 very high speed of suprathermal electrons) as is the case here with the reconnection region being
182 located all the way above the cusp in the opposite, southern hemisphere. Field line (3) shows heated
183 electrons also coming from the north (southward red arrow) because it is reconnected there also (field
184 line (3) is doubly reconnected), but field line (2) shows pristine (cold, blue arrow) electrons coming
185 from the north because this field line has not reconnected (yet) at this end. Depending on the timing
186 of magnetic field line reconnection at both locations, as the spacecraft traverses the magnetopause it
187 typically observes heated solar wind electrons streaming in both parallel and anti-parallel directions
188 outside the magnetopause on doubly reconnected field lines (field line (3)) as well as unidirectional
189 heated electrons which signal singly reconnected field lines (field line (2)). The latter unidirectional
190 heated electrons are observed on the outermost, sunward side of this boundary layer. Although not
191 detailed here, the newly closed field lines eventually sink into the magnetosphere and form broad
192 boundary layers inside the magnetopause (e.g., Lavraud et al., 2006; 2018; Øieroset et al., 2008). In
193 other words, crossing the magnetopause from any given side one expects to observe a very complex,
194 layered structure with variable particle properties corresponding to the mixing of particles from both
195 sides (such complex signatures are observed at Earth also at other energies and for other species).

196 The double reconnection scenario of heliospheric and VLISM field lines unveiled in the simulation
197 of Figure 1b should similarly lead to specific particle signatures in the broad vicinity of the
198 heliopause. Such topological considerations have been put forth to explain the fact that the drop in
199 ACR fluxes is not collocated (it occurs further outside) with the main magnetic field increase at the
200 Voyager 1 and 2 heliopause crossings (e.g., Krimigis et al., 2013; Fuselier et al., 2020). Because
201 ACRs are produced within the Heliosphere, their drop outside the reported heliopause crossings (as
202 well as the timings and anisotropies of various species at different energies) is taken as evidence of
203 particle leakage due to reconnected field lines in the vicinity of the heliopause, but remote from
204 Voyager 1 and 2 (e.g., Fuselier et al., 2020), or other instabilities (cf. introduction). But the complete
205 disappearance (in all directions) of ACRs has also been interpreted as an escape (in both parallel and

206 anti-parallel directions) along doubly reconnected field lines as shown in Figure 1b (since the ACRs
207 originate inside the Heliosphere). In this scenario, even past the drop in ACRs, the Voyager 1 and 2
208 spacecraft would remain magnetically connected to an open heliopause and thus remain inside the
209 main current sheet that would signal the effective transition into the pristine VLISM (e.g., Fisk and
210 Gloeckler, 2022; Turner et al., 2022). Particle measurements with complete directionality information
211 are critical to fully investigate the large-scale heliopause magnetic topology.

212 To first order, the analogy between Figures 1a and 1b stops at the fact that the same field lines may
213 reconnect twice at widely separated distances (when conditions at the nose are not favorable for
214 reconnection to occur there). This is because the signatures in terms of magnetic field (pile-up,
215 orientation) and particles species, energies, and anisotropies are widely different in both contexts
216 (different particle sources, coexistence of multiple populations (e.g., PUIs), magnetic geometries,
217 system size, presence/absence of shocks, instabilities at play, etc.). As further discussed in the next
218 section, the width of these possible heliopause boundary layers, although not known, could be
219 substantial. Furthermore, the non-vanishing outward radial flow observed at both Voyager 1 and 2
220 near the heliopause is not consistent with most models, and comparison to the Earth's magnetosphere
221 does not provide insight in that respect. Determining where reconnection occurs, how plasma flows
222 near the heliopause, and the ensuing large-scale magnetic topology requires more complete
223 observations, in particular in the few eV to few tens-of-keV range (thermal and PUI). These are
224 critical to better define the heliopause, its location and its shape.

225 Finally, it should be noted that magnetic reconnection along the heliopause has been proposed as one
226 of the possible mechanisms to explain the ribbon structure of energetic neutral atom fluxes in global
227 observations from the Interstellar Boundary Explorer (IBEX). However, given the alternating polarity
228 structure of the heliospheric magnetic field along significant portions of the heliopause it is unclear
229 how this process could explain the configuration and steadiness of the ribbon (McComas et al., 2009;
230 2011). The latter point has another important implication, and that is that the locations of magnetic
231 reconnection on the heliopause surface, and therefore the large-scale magnetic topology of the
232 heliopause, should change over the course of the solar cycle given the alternating magnetic field
233 polarity.

234 **2.3 What are reconnection properties in outer heliospheric regimes?**

235 The plasma properties of the outer heliosphere differ greatly from those of the inner heliosphere
236 where magnetic reconnection has been widely studied. In particular, the pressure in the accumulated
237 PUIs becomes larger than the solar wind thermal pressure already upstream of the termination shock,
238 and at the termination shock the pickup ions are heated more than the thermal solar wind (Richardson
239 et al., 2008; Mostafavi et al., 2017; 2018). The plasma Beta conditions also largely change in the
240 outer Heliosphere, past the termination shock, at and beyond the heliopause in the VLISM. Also,
241 while asymmetric reconnection should be expected at the heliopause, symmetric reconnection may be
242 occurring at current sheets in the inner (Drake et al., 2017) and outer heliosheath, as well as in the
243 VLISM (although surprisingly no evidence has been reported for reconnection in the inner
244 heliosheath so far, and in the VLISM current sheets are expected to be much less frequent). Studying
245 magnetic reconnection in all these regions would thus provide significant new insights into our
246 understanding of magnetic reconnection in new plasma regimes.

247 For example, concerning the inner heliosheath, Opher et al. (2011) proposed that the magnetic field
248 and flows are not laminar, but instead consist of magnetic islands that develop upstream at the
249 heliopause through reconnection (see also Schwadron and McComas (2013) regarding flux ropes at

250 the heliopause). As discussed above the location of reconnection at the heliopause remains unclear,
251 but it has been suggested that large pressure gradients across the heliopause due to PUIs produce a
252 diamagnetic drift that may stabilize magnetic reconnection. This adds to the low magnetic shear
253 observed at the Voyager 1 and 2 crossings, which likely precludes reconnection from occurring
254 locally at the nose (Swisdak et al., 2010, 2013; Fuselier and Cairns, 2017; Opher et al., 2017; Fuselier
255 et al., 2020). Magnetic reconnection may, however, develop at other locations on the flanks of the
256 heliopause where conditions are satisfied thanks to higher magnetic shear (Opher et al., 2017).

257 Near the Earth's magnetosphere and in the solar wind, where high accuracy thermal plasma
258 measurements are available, detailed studies of the energy conversion and partitioning associated
259 with reconnection can be made (e.g., Burch et al., 2016). Although there are obvious payload
260 limitations compared to near-Earth missions, studying such questions in the vastly different outer
261 heliosphere regimes would require dedicated low energy thermal plasma measurements, including
262 PUIs, on a future Interstellar Probe. Studying the properties of reconnection in different regimes
263 would also benefit from different types of wave measurements. This is true for example for the study
264 of wave – particle interactions, but also because wave data can provide complementary
265 measurements of plasma moments (such as density, as has been done on Voyager 1 and 2 in the
266 absence of density measurement from thermal particle measurements (e.g., Gurnett and Kurth 2017;
267 Kurth and Gurnett, 2020)).

268 **2.4 How thick are reconnection boundary layers at the Heliopause?**

269 Using again an analogy with the Earth's magnetopause: the timing, location, geometry and rate of
270 magnetic reconnection should produce various layers of different widths as a function of species,
271 energy and pitch angle. These boundary layers are not solely confined to one side (i.e.,
272 magnetosheath boundary layer marked on the outside of the magnetopause in Figure 1a), but rather
273 are present on both sides of the current sheet (solar wind populates boundary layers on the inside of
274 the magnetopause and the entire cusp region). If magnetic reconnection affects the topology of the
275 heliopause on very large scales as illustrated in the simulation of Figure 1b, there is no doubt that
276 significant effects in particle and field properties should be observed near the heliopause, but also
277 possibly up to large distances although that remains unknown.

278 Indeed, the widths of the reconnection boundary layers on both sides of the current sheet depend on
279 the reconnection rate (which depends on local plasma properties), on the distance from the
280 reconnection region, as well as on the profile in Alfvén speed along the field lines as the reconnection
281 kinks propagate on either side of the boundary. Again, the expected widths of the layers remain
282 unclear for the heliopause. Some studies propose rather thin boundary layers, based on particle
283 properties around the heliopause (Fuselier and Cairns, 2017; Fuselier et al., 2020). But other studies
284 suggest the observed ACR leakage is actually occurring well inside the actual heliopause (which
285 would not be crossed yet), in a much broader inner heliopause boundary layer that results from a
286 reconnection process akin to that depicted in Figure 1b (e.g., Fisk and Gloeckler, 2016; 2022; Turner
287 et al., 2022). Again, in an analogy to the case of the Earth depicted in Figure 1a, it should be noted
288 that the boundary layer that forms on the Earthward side (the high magnetic field side) of the
289 magnetopause as a result of the process of double magnetic reconnection is typically of the order of 1
290 Earth radius, which is a significant size compared to the scale size of the dayside magnetosphere
291 (~10% of the ~10 Earth radii magnetopause stand-off distance). If similar types of boundary layers
292 were forming at the heliopause, they could be of very significant extents, possibly tens of AUs inside
293 or outside the heliopause (depending on its definition). However, we lack the appropriate
294 measurements on Voyager 1 and 2, particularly thermal plasma properties, to undoubtedly estimate

295 the key parameters and decipher the complex structuring of all the expected types of boundary layers
296 and their extents.

297 **2.5 What are the roles of magnetic field draping and pile-up processes?**

298 Boundary layers produced by magnetic reconnection are often intricately linked to draping and pile-
299 up processes. This is true at the Earth's magnetopause and is likely also true at the heliopause.
300 Draping has been proposed to occur in the outer heliosheath, outside the heliopause, with an
301 associated magnetic pile-up and plasma depletion region (e.g., Gurnett et al., 1993; Schwadron et al.,
302 2009; Fuselier et al., 2020; Kornbleuth et al., 2021; Mostafavi et al., 2022), the thickness of which
303 has been estimated as ~ 5 AU (Fuselier and Cairns, 2013). The location of the plasma depletion layer
304 has been proposed to be displaced from the nose, unlike at Earth, based on calculations that account
305 for the different partitioning between thermal, kinetic and magnetic pressures in a high Beta
306 environment (Fuselier and Cairns, 2013). As is the case for the Earth's magnetosphere, the width,
307 extent and location of this layer may impact where reconnection is triggered, as well as the stability
308 of the reconnection process (Fuselier et al., 2000; Lavraud et al., 2005). An open question regarding
309 these layers, however, is that while Gurnett et al., (2013) first reported densities of $\sim 0.09\text{--}0.11\text{ cm}^{-3}$
310 past the heliopause, higher densities up to $\sim 0.14\text{ cm}^{-3}$ were actually measured at distances ~ 20 AU
311 beyond, as reported in Gurnett and Kurth (2017) and Kurth and Gurnett (2020) for both Voyager
312 spacecraft.

313 A plasma depletion layer has also been studied (Izmodenov and Alexashov 2015) on the inside of the
314 heliopause. As for the outer heliosheath pile-up region, the magnetic field pile-up forms gradients
315 that decelerate and deflect plasma flows around and to the side of the obstacle formed by the
316 heliopause. As a result, plasma density is depleted from the middle of the inner heliosheath to the
317 heliopause. However, the effects of charge exchange between interstellar ions and neutrals should be
318 significant and affect plasma flows and density depletion both inside and outside the heliopause.
319 How these plasma depletion and magnetic pile-up layers develop and affect the interactions at the
320 heliopause remain open questions. Proper low energy plasma measurements are required to address
321 these questions.

322 Finally, using MHD simulations Opher and Drake (2013) suggested that the draping outside the
323 heliopause is strongly affected by the solar magnetic field, although underlying physical mechanism
324 was not understood. They showed that as the VLISM magnetic field approaches the heliopause, it
325 twists and acquires an east–west component, an effect that did not occur if the solar magnetic field
326 was not present in the simulation. This draping could explain the twist of the magnetic field and the
327 unexpectedly low magnetic shear at Voyager 1 and Voyager 2 (cf. also Grygorczuk et al. 2014;
328 Isenberg et al. 2015; Opher et al., 2017). This possibility, however, remains to be confronted by
329 observations and such observations, in particular in terms of low energy particles, are lacking.

330 **3 Measurement requirements**

331 A dedicated outer heliosphere and interstellar space mission is required to understand the interaction
332 of our heliosphere with the VLISM at the heliopause, as proposed in McNutt et al. (2022) and Brandt
333 et al. (2022). The Mission Concept study Report (MCR) may be found at
334 <https://interstellarprobe.jhuapl.edu/Interstellar-Probe-MCR.pdf>.

335 **3.1 Main measurement requirements for studying reconnection at the heliopause**

336 To tackle science questions related to reconnection at the heliopause, a number of important and
337 complementary measurements are needed on such a mission. These include magnetic field, plasma
338 wave, suprathermal and energetic particles (up to ACR and GCR energies) instruments (since such
339 are available on Voyager 1 and 2 they are not the focus of this WP), but also importantly low energy
340 particle measurements that are not present onboard Voyager 1 and 2 (although operating the Faraday
341 Cups do not have appropriate fields-of-view (FoV) on Voyager 2 at and beyond the heliopause).
342 Low-energy particle measurements should cover the few-eV to few-tens-of-keV range, which include
343 the thermal solar wind, heliosheath and VLISM populations, as well as PUIs. Other science questions
344 and requirements related to PUIs are addressed in other WPs. We thus focus on measurement
345 requirements for the lowest energy thermal populations here.

346 **3.2 Basic thermal plasma measurement requirements**

347 Bulk flow and thermal energies of low energy ions and electrons typically fall in the following ranges
348 as a function of regions: solar wind from a few eV to 20 keV, inner heliosheath from eV to keV and
349 outer heliosheath and VLISM are likely only in the few eV range, although this is not well
350 constrained (e.g., Zank, 2015). Interstellar Probe shall fly further than 200 AU (possibly beyond 400
351 AU) into interstellar space. This leads to constraints in terms of requirements and design, the most
352 critical being as follows:

- 353 • Ion and electron populations range from the dense solar wind at 1 AU to the very tenuous
354 ionized medium at 200 AU and beyond, with a factor 10^{-6} lower fluxes/count rates expected.
355 Measurements thus require low noise, high dynamic range detectors.
- 356 • The instrument shall be designed to work for at least 50 years. Technologies (electronics
357 components) and detectors should have comparable life-time expectancies.
- 358 • Sampling time resolution should range from second (inner heliosphere) to hour (VLISM) time
359 scales. Control and commanding (firmware), as well as onboard computations and packaging shall
360 handle a large dynamic range of modes and operation cycles.

361 Two types of instruments can be foreseen to address these requirements, in a complementary fashion:
362 Faraday cup (FC) and electrostatic analyzer (ESA). Having both would permit important redundancy
363 of parts of the critical measurements (basic moments of the distribution function such as density,
364 velocity and temperatures).

365 **3.3 Faraday cup requirements**

366 FCs are simpler in design and require fewer resources. FCs have proven to be a robust design for
367 long term use on many missions, as for example on Voyager 2. An advantage of FCs is that it is
368 straightforward to increase their geometry factor, as would be critical to detect low plasma densities.
369 FCs are typically designed for measuring low energy ions, but given the low cadences required in the
370 outer heliosphere the FCs for an interstellar mission should also include an electron mode. Because
371 the spacecraft is expected to be spin-stabilized, three to four FC heads with appropriate FoV should
372 be sufficient to make three-dimensional sampling and provide appropriate plasma moments. Each
373 head may be sectorized to perform flow measurements. FCs have naturally a low response to noise
374 from energetic particles, as these do not provide a significant current. But appropriate electronics
375 should be used to suppress internal noise sources, and accurate high-voltage power supplies should
376 be designed for the very low energies of the inner and outer heliosheath and VLISM.

377 **3.4 Electrostatic analyzer requirements**

378 An ESA instrument is fundamental as it provides information on the full particle distribution function
 379 (temperature anisotropies, pitch angles measurements, easier separation of species, etc.). It should
 380 have a 360° planar FoV (possibly 180°) and measure the full three-dimensional distribution function
 381 thanks to the spacecraft spin. A critical design aspect for that type of instrument concerns the high
 382 dynamic range of fluxes expected, which impacts the type of detector – Channel Electron Multipliers
 383 or Micro-Channel Plates – that should be used. While the former is typically more robust with time
 384 (lifetime) and has higher intrinsic dynamic range, the latter requires significantly lower resources
 385 (power). Another critical design aspect for such type of instrument is the signal-to-noise ratio, which
 386 owing to penetrating radiation and electronics clearly will require appropriate mitigation measures.
 387 An obvious concept to be used is a coincidence scheme, which should allow to reduce system
 388 background noise down to $< 10^{-4} \text{ s}^{-1}$

389 As for the FCs, the ESA should be designed with low noise electronics and accurate high-voltage
 390 supply system down to low voltages (3 eV baseline, which is consistent with measurements to below
 391 the expected spacecraft potential of + 5 V). To save significant resources, the instrument ideally
 392 should be able to measure both ions and electrons with the same detector head. State-of-the-art
 393 methods should be designed to perform such alternated measurements of ions and electrons to
 394 optimize front-end and high-voltage resources. Performing such alternated measurements of ions and
 395 electrons does not impact science requirements since measurement cadences do not need to be high
 396 in the outer heliosphere and VLISM.

397 **3.5 Additional notes on designs**

398 The ESA instrument may be designed with a Time-of-Flight system to perform composition
 399 measurements down to low energies. In such a case, a clever design would be needed to perform both
 400 ions and electrons with the same head. Alternatively, half of the 360° FoV could be devoted to
 401 electrons and the other for ions. Or yet two separate heads/instruments could be used to ensure that
 402 ion composition is performed. It may be argued, however, that a low energy ESA instrument could
 403 be limited to measuring all ions without composition, but yet providing some composition
 404 information through energy separation (if the bulk flow is larger than the thermal speed), given that a
 405 dedicated PUI instrument with composition is required anyway and may go down to complementary
 406 low energies. While a PUI instrument could have limited angular resolution (e.g., 22.5°), an ESA
 407 instrument dedicated to the solar wind and VLISM should ideally have higher angular resolution (\leq
 408 10°), at least in appropriate portions of the FoV. This aspect requires more detailed trade-off studies
 409 to find the appropriate design. Finally, we shall also note that the ESA instrument could be designed
 410 with a deflection system at the entrance to increase the FoV of the instrument when the spacecraft
 411 will be three-axis stabilized during planetary fly-bys, but this would be at the expense of reasonable,
 412 but non-negligible resources. We remind that more details on the measurement requirements
 413 (resolutions in energy, angle, time, mass etc.) are provided in the Mission Concept study Report
 414 (MCR) at <https://interstellarprobe.jhuapl.edu/Interstellar-Probe-MCR.pdf>.

415 **4 Conflict of Interest**

416 The authors declare that the research was conducted in the absence of any commercial or financial
 417 relationships that could be construed as a potential conflict of interest.

418 **5 Author Contributions**

419 All authors have contributed in various ways to the content of this article and agree to its content.

420 **6 Funding**

421 Work performed at LAB and IRAP in France were supported by CNES, CNRS, and the Universities
422 of Bordeaux and Toulouse. The work at JHU/APL was supported also by NASA under contracts
423 NAS5 97271, NNX07AJ69G, and NNN06AA01C and by subcontract at the Office for Space
424 Research and Technology.

425 **7 Acknowledgments**

426 The authors are grateful to the Voyager and Interstellar Probe mission teams that have, and will
427 continue, making the science discussed in this article possible. The authors additionally acknowledge
428 valuable discussions with the Cassini/MIMI and SHIELD DRIVE Science Center teams.

429 **8 Data Availability Statement**

430 The present work does not involve the use of any specific data that needs referencing.

431 **9 References**

432 Borovikov, S., and N. Pogorelov, *The Astrophysical Journal Letters*, Volume 783, Issue 1, article id.
433 L16, 6 pp., <https://doi.org/10.1088/2041-8205/783/1/L16> (2014).

434 Brandt, P. C., et al., *Acta Astronautica*, <https://doi.org/10.1016/j.actaastro.2022.07.011> (2022).

435 Burch et al., *Space Science Reviews*, Volume 199, Issue 1-4, pp. 5-21,
436 <https://doi.org/10.1007/s11214-015-0164-9> (2016).

437 Burlaga et al., *Science*, Volume 341, Issue 6142, pp. 147-150,
438 <https://doi.org/10.1126/science.1235451> (2013).

439 Burlaga, L. F. and N. F. Ness, *The Astrophysical Journal*, Volume 829, Issue 2, article id. 134, 10
440 pp., <https://doi.org/10.3847/0004-637X/829/2/134> (2016).

441 Burlaga, L. F., et al., *Nature Astronomy*, Volume 3, p. 1007-1012, <https://doi.org/10.1038/s41550-019-0920-y> (2019).

443 Cairns, I. H., and S. A. Fuselier, *The Astrophysical Journal*, Volume 834, Issue 2, article id. 197, 11
444 pp., <https://doi.org/10.3847/1538-4357/834/2/197> (2017).

445 Cummings, A. C., et al., *The Astrophysical Journal*, Volume 906, Issue 2, id.126, 15 pp.,
446 <https://doi.org/10.3847/1538-4357/abc5c0> (2021).

447 Decker, R. B., et al. *Science*, Volume 309, Issue 5743, pp. 2020-2024,
448 <https://doi.org/10.1126/science.1117569> (2005).

449 Decker, R. B., et al., *Nature*, Volume 454, Issue 7200, pp. 67-70, <https://doi.org/10.1038/nature07030>
450 (2008).

- 451 Decker, R. B., et al., *Nature*, Volume 489, Issue 7414, pp. 124-127,
452 <https://doi.org/10.1038/nature11441> (2012).
- 453 Dialynas, K., et al., *Geophysical Research Letters*, Volume 46, Issue 14, pp. 7911-7919,
454 <https://doi.org/10.1029/2019GL083924> (2019).
- 455 Dialynas, K., et al., *The Astrophysical Journal Letters*, Volume 905, Issue 2, id.L24, 7 pp.,
456 <https://doi.org/10.3847/2041-8213/abcaaa> (2020).
- 457 Dialynas, K., et al., *The Astrophysical Journal*, Volume 917, Issue 1, id.42, 8 pp.,
458 <https://doi.org/10.3847/1538-4357/ac071e> (2021).
- 459 Dialynas, K., et al., *Space Science Reviews*, Volume 218, Issue 4, article id.21,
460 <https://doi.org/10.1007/s11214-022-00889-0> (2022).
- 461 Drake, J. F., et al., *The Astrophysical Journal*, Volume 837, Issue 2, article id. 159, 9 pp.,
462 <https://doi.org/10.3847/1538-4357/aa6304> (2017).
- 463 Fisk, L. A., and G. Gloeckler, *The Astrophysical Journal*, Volume 789, Issue 1, article id. 41, 9 pp.,
464 <https://doi.org/10.1088/0004-637X/789/1/41> (2014).
- 465 Fisk, L. A., and G. Gloeckler, *Journal of Physics: Conference Series*, Volume 767, Issue 1, article id.
466 012008, <https://doi.org/10.1088/1742-6596/767/1/012008> (2016).
- 467 Fisk, L. A., and G. Gloeckler, *The Astrophysical Journal*, Volume 927, Issue 1, id.73, 11 pp.,
468 <https://doi.org/10.3847/1538-4357/ac4d2f> (2022).
- 469 Florinski, V., et al., *Journal of Geophysical Research: Space Physics*, Volume 110, Issue A7, CiteID
470 A07104, <https://doi.org/10.1029/2004JA010879> (2005).
- 471 Florinski, V., *The Astrophysical Journal*, Volume 813, Issue 1, article id. 49, 8 pp.,
472 <https://doi.org/10.1088/0004-637X/813/1/49> (2015).
- 473 Fuselier, S. A., et al., *Geophysical Research Letters*, Volume 27, Issue 4, p. 473-476,
474 <https://doi.org/10.1029/1999GL003706> (2000).
- 475 Fuselier, S. A., and I. H. Cairns, *The Astrophysical Journal*, Volume 771, Issue 2, article id. 83, 10
476 pp., <https://doi.org/10.1088/0004-637X/771/2/83> (2013).
- 477 Fuselier, S. A., and I. H. Cairns, *Journal of Physics: Conference Series*, Volume 900, Issue 1, article
478 id. 012007, <https://doi.org/10.1088/1742-6596/900/1/012007> (2017).
- 479 Fuselier, S. A., et al., *Journal of Physics: Conference Series*, Volume 1620, Issue 1, article id.
480 012004, <https://doi.org/10.1088/1742-6596/1620/1/012004> (2020).
- 481 Fuselier, S. A., et al., *The Astrophysical Journal Letters*, Volume 915, Issue 2, id.L26, 8 pp.,
482 <https://doi.org/10.3847/2041-8213/ac0d5c> (2021).
- 483 Giacalone, J., et al. *Space Science Reviews*, Volume 218, Issue 4, article id.22,
484 <https://doi.org/10.1007/s11214-022-00890-7> (2022).

- 485 Gloeckler, G., et al., *Journal of Geophysical Research*, Volume 99, Issue A9, p. 17637-17644,
486 <https://doi.org/10.1029/94JA01509> (1994).
- 487 Gloeckler, G. and L. A. Fisk, *The Astrophysical Journal Letters*, Volume 806, Issue 2, article id. L27,
488 5 pp., <https://doi.org/10.1088/2041-8205/806/2/L27> (2015).
- 489 Gosling, J. T., et al., *Geophysical Research Letters*, Volume 17, Issue 11, Pages 1833-1836,
490 <https://doi.org/10.1029/GL017i011p01833> (1990).
- 491 Grygorczuk, J., et al., *The Astrophysical Journal Letters*, Volume 789, Issue 2, article id. L43, 4 pp.,
492 <https://doi.org/10.1088/2041-8205/789/2/L43> (2014).
- 493 Gurnett, D. A., et al., *Science*, Volume 341, Issue 6153, pp. 1489-1492,
494 <https://doi.org/10.1126/science.1241681> (2013).
- 495 Gurnett, D. A. and W. S. Kurth, *Nature Astronomy*, Volume 3, p. 1024-1028,
496 <https://doi.org/10.1038/s41550-019-0918-5> (2019).
- 497 Hesse, M., and P. A. Cassak, *Journal of Geophysical Research*, Volume 125, Issue 2,
498 <https://doi.org/10.1029/2018JA025935> (2019).
- 499 Holzer, T. E., *Journal of Geophysical Research*, Volume 77, Issue 28, p. 5407,
500 <https://doi.org/10.1029/JA077i028p05407> (1972).
- 501 Isenberg, P. A., et al., *The Astrophysical Journal*, Volume 805, Issue 2, article id. 153, 10 pp.,
502 <https://doi.org/10.1088/0004-637X/805/2/153> (2015).
- 503 Izmodenov, V. V., et al., *Space Science Reviews*, Volume 146, Issue 1-4, pp. 329-351,
504 <https://doi.org/10.1007/s11214-009-9528-3> (2009)
- 505 Izmodenov, V. V., and D. B. Alexashov, *The Astrophysical Journal Supplement Series*, Volume 220,
506 Issue 2, article id. 32, 14 pp., <https://doi.org/10.1088/0067-0049/220/2/32> (2015).
- 507 Jokipii, J. R., and J. Giacalone, *Space Science Reviews*, v. 83, Issue 1/2, p. 123-136 (1998).
- 508 Kivelson, M. G., and C. T. Russell, *Introduction to space physics*, Cambridge university Press,
509 <https://doi.org/10.1017/9781139878296> (1995).
- 510 Kleimann, J., et al., *Space Science Reviews*, Volume 218, Issue 4, article id.36,
511 <https://doi.org/10.1007/s11214-022-00902-6> (2022).
- 512 Kornbleuth, M., et al., *The Astrophysical Journal*, Volume 923, Issue 2, id.179, 13 pp.,
513 <https://doi.org/10.3847/1538-4357/ac2fa6> (2021).
- 514 Korolkov, S., et al., *Journal of Physics: Conference Series*, Volume 1640, Issue 1, article id. 012012,
515 <https://doi.org/10.1088/1742-6596/1640/1/012012> (2020).
- 516 Krimigis, S. M., et al., *Nature*, Volume 474, Issue 7351, pp. 359-361,
517 <https://doi.org/10.1038/nature10115> (2011).

- 518 Krimigis, S. M., et al., *Science*, Volume 341, Issue 6142, pp. 144-147,
519 <https://doi.org/10.1126/science.1235721> (2013).
- 520 Krimigis, S. M., et al., *Nature Astronomy*, Volume 3, p. 997-1006, [https://doi.org/10.1038/s41550-](https://doi.org/10.1038/s41550-019-0927-4)
521 [019-0927-4](https://doi.org/10.1038/s41550-019-0927-4) (2019).
- 522 Kurth, W. S., and D. A. Gurnett, *The Astrophysical Journal Letters*, Volume 900, Number 1,
523 <https://doi.org/0.3847/2041-8213/abae58> (2020).
- 524 Lavraud, B., et al., *Journal of Geophysical Research: Space Physics*, Volume 110, Issue A2, CiteID
525 A02209, <https://doi.org/10.1029/2004JA010804> (2005).
- 526 Lavraud, B., et al., *Journal of Geophysical Research: Space Physics*, Volume 111, Issue A5, CiteID
527 A05211, <https://doi.org/10.1029/2005JA011266> (2006).
- 528 Lavraud, B., et al., *Journal of Geophysical Research: Space Physics*, Volume 123, 5407–5419,
529 <https://doi.org/10.1029/2017JA025152> (2018).
- 530 Lavraud, B., et al., *Bulletin of the American Astronomical Society (BAAS)*, Pending doi (2022).
- 531 McComas, D. J., et al. (2009), *Science*, 326, 959, <https://doi.org/10.1126/science.1180906> (2009).
- 532 McComas, D. et al., *Geophysical Research Letters*, Volume38, Issue18,
533 <https://doi.org/10.1029/2011GL048763> (2011).
- 534 McComas, D., and N. Schwadron, *The Astrophysical Journal Letters*, Volume 795, Issue 1, article id.
535 L17, 3 pp., <https://doi.org/10.1088/2041-8205/795/1/L17> (2014).
- 536 McComas, D. J., et al., *The Astrophysical Journal Supplement Series*, Volume 254, Issue 1, id.19, 17
537 pp., <https://doi.org/10.3847/1538-4365/abee76> (2021).
- 538 McNutt, R. L., et al., *Acta Astronautica*, 196: 13-28, <https://doi.org/10.1016/j.actaastro.2022.04.001>
539 (2022).
- 540 Mostafavi, P., et al., *The Astrophysical Journal*, Volume 841, Issue 1, article id. 4, 16 pp.,
541 <https://doi.org/10.3847/1538-4357/aa6f10> (2017).
- 542 Mostafavi, P., et al., *The Astrophysical Journal*, Volume 868, Issue 2, article id. 120, 13 pp.,
543 <https://doi.org/10.3847/1538-4357/aab91> (2018).
- 544 Mostafavi, P., et al., *Space Science Reviews*, Volume 218, Issue 4, article id.27,
545 <https://doi.org/10.1007/s11214-022-00893-4> (2022).
- 546 Øieroset, M., et al., *Geophysical Research Letters*, 35, L17S11.
547 <https://doi.org/10.1029/2008GL033661> (2008).
- 548 Opher, M., et al., *The Astrophysical Journal*, Volume 734, Issue 1, article id. 71, 10 pp.,
549 <https://doi.org/10.1088/0004-637X/734/1/71> (2011).
- 550 Opher, M., and J. F. Drake, *The Astrophysical Journal Letters*, Volume 778, Issue 2, article id. L26, 6
551 pp., <https://doi.org/10.1088/2041-8205/778/2/L26> (2013).

- 552 Opher, M., et al., *The Astrophysical Journal Letters*, Volume 839, Issue 1, article id. L12, 6 pp.,
553 <https://doi.org/10.3847/2041-8213/aa692f> (2017).
- 554 Opher, M., et al., *Nature Astronomy*, Volume 4, p. 675-683, [https://doi.org/10.1038/s41550-020-](https://doi.org/10.1038/s41550-020-1036-0)
555 1036-0 (2020).
- 556 Opher, M., et al., *The Astrophysical Journal*, Volume 922, Issue 2, id.181, 12 pp.,
557 <https://doi.org/10.3847/1538-4357/ac2d2e> (2021).
- 558 Pierrard, V., et al., *Frontiers in Astronomy and Space Sciences*, Volume 8, id.69,
559 <https://doi.org/10.3389/fspas.2021.681401> (2021)
- 560 Richardson, J. D., et al., *Nature*, Volume 454, Issue 7200, pp. 63-66,
561 <https://doi.org/10.1038/nature07024> (2008).
- 562 Richardson, J. D., et al., *Nature Astronomy*, Volume 3, p. 1019-1023,
563 <https://doi.org/10.1038/s41550-019-0929-2> (2019).
- 564 Richardson, J. D., et al., *The Astrophysical Journal Letters*, Volume 919, Issue 2, id.L28, 6 pp.,
565 <https://doi.org/10.3847/2041-8213/ac27b1> (2021).
- 566 Richardson, J. D., et al., *Space Science Reviews*, Volume 218, Issue 4, article id.35
567 <https://doi.org/10.1007/s11214-022-00899-y> (2022).
- 568 Ruderman, M. S., and H. J. Fahr, *Astronomy and Astrophysics*, Vol. 275, p. 635 (1993).
- 569 Schwadron, N. A., and D. J. McComas, *AIP Conference Proceedings*, Volume 858, pp. 165-170,
570 <https://doi.org/10.1063/1.2359322> (2006).
- 571 Schwadron, N. A., and D. J. McComas, *The Astrophysical Journal Letters*, Volume 778, Issue 2,
572 article id. L33, 5 pp., <https://doi.org/10.1088/2041-8205/778/2/L33> (2013).
- 573 Schwadron, N. A., et al., *Science*, Volume 326, Issue 5955, pp. 966,
574 <https://doi.org/10.1126/science.1180986> (2009).
- 575 Stone, E. C., et al., *Science*, Volume 309, Issue 5743, pp. 2017-2020,
576 <https://doi.org/10.1126/science.1117684> (2005).
- 577 Stone, E. C., et al., *Nature*, Volume 454, Issue 7200, pp. 71-74, <https://doi.org/10.1038/nature07022>
578 (2008).
- 579 Stone, E. C., et al., *Science*, Volume 341, Issue 6142, pp. 150-153,
580 <https://doi.org/10.1126/science.1236408> (2013).
- 581 Stone, E. C., et al., *Nature Astronomy*, Volume 3, p. 1013-1018, [https://doi.org/10.1038/s41550-019-](https://doi.org/10.1038/s41550-019-0928-3)
582 0928-3 (2019).
- 583 Strauss, R. D., et al., *Astronomy and Astrophysics*, Volume 522, id.A35, 8 pp,
584 <https://doi.org/10.1051/0004-6361/201014528> (2010).

585 Strumik, M., et al., The Astrophysical Journal, Volume 782, Issue 1, article id. L7, 5 pp.,
 586 <https://doi.org/10.1088/2041-8205/782/1/L7> (2014).

587 Swisdak, M., J. F. Drake, M. Opher and A. Bibi, The Astrophysical Journal, Volume 710, Issue 2,
 588 pp. 1769-1775, <https://doi.org/0.1088/0004-637X/710/2/1769> (2010).

589 Swisdak, M., J.F. Drake, and M. Opher, The Astrophysical Journal Letters, Volume 774, Issue 1,
 590 article id. L8, 5 pp., <https://doi.org/10.1088/2041-8205/774/1/L8> (2013).

591 Turner, D. L., et al., Evidence of a Thick Heliopause Boundary Layer Resulting from Active
 592 Magnetic Reconnection with the Interstellar Medium, 2022, in preparation.

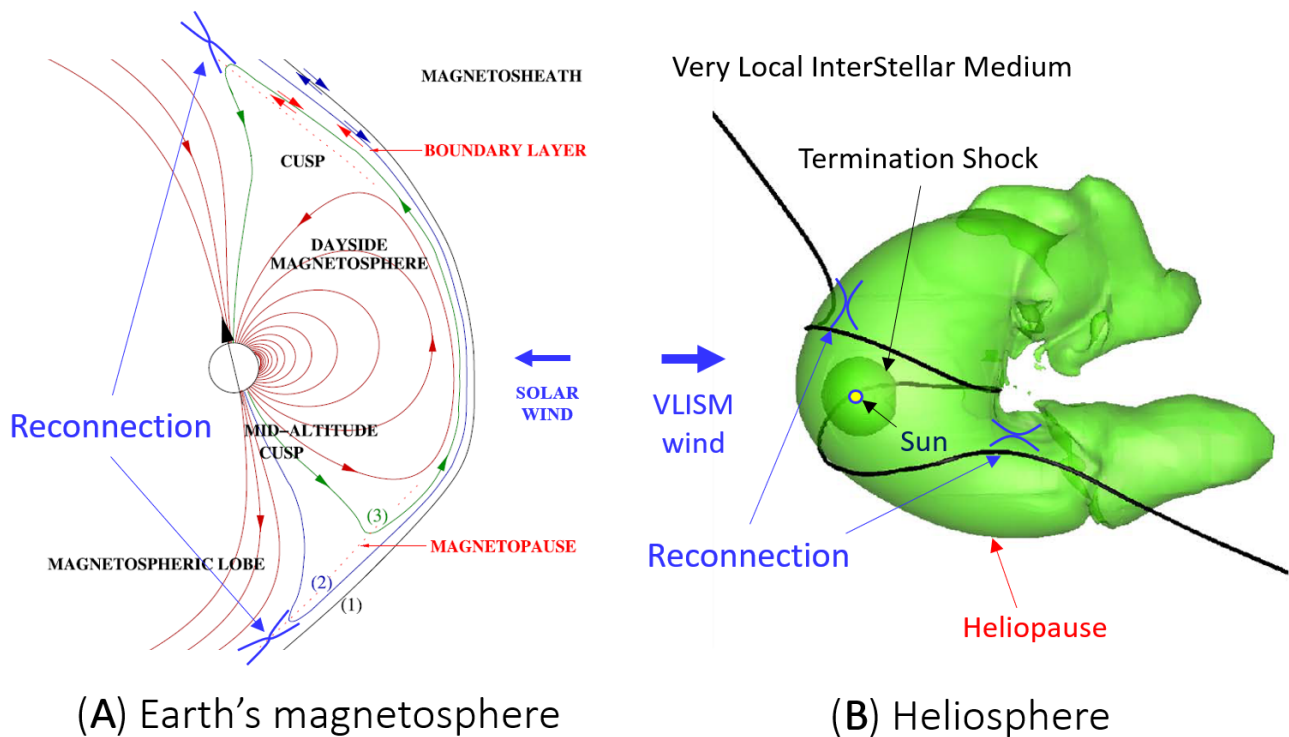
593 Webber, W. R., and F. B. McDonald, Geophysical Research Letters, Volume 40, Issue 9, pp. 1665-
 594 1668, <https://doi.org/10.1002/grl.50383> (2013).

595 Zank, G. P., Annual Review of Astronomy and Astrophysics, Volume 53, pp 449-500,
 596 <https://doi.org/10.1146/annurev-astro-082214-122254> (2015).

597 Zirnstein, E. J., et al., Space Science Reviews, Volume 218, Issue 4, article id.28,
 598 <https://doi.org/10.1007/s11214-022-00895-2> (2022)

599

600 **10 Figure captions**



601

602 **Figure 1.** (A) Earth's dayside topology when magnetic fields are parallel at the nose of the
 603 magnetosphere, leading to complex boundary layers inside (cusp) and outside (magnetosheath) the
 604 magnetopause (red dotted line) as a result of reconnection occurring twice and sequentially on the

605 same magnetic field line. Blue arrows adjacent to field lines (1) and (2) illustrate the presence and
606 direction of streaming, cold solar wind electrons. Red arrows, on field lines (2) and (3), correspond to
607 streaming heated electrons. Field line (1) is a pristine field line open to the solar wind at both ends.
608 Field line (2) is a field line which has reconnected in only one hemisphere. Field line (3) has
609 reconnected in both hemispheres. Adapted from Lavraud et al. (2006). **(B)** MHD simulation result of
610 the heliospheric interaction with the Very Local Interstellar Medium (VLISM). The heliopause is
611 approximated with an isocontour in temperature (green shading). A magnetic field lines is shown in
612 black. It results from double reconnection of a VLISM field line (straight extensions of the field line
613 to the top and bottom) with the wound field (spiral) of the heliosphere. Adapted from Opher et al.
614 (2017).